

## Simulation of Stress Distribution on the Upper First Molar and Alveolar Bone with the Transpalatal Arch and Upper Second Molar Using Finite Element Analysis

Presti Bhakti Pratiwi<sup>1</sup>, Retno Widayati<sup>2</sup>, Maria Purbiati<sup>3</sup>

<sup>1</sup>Department of Orthodontics, Faculty of Dentistry, Universitas Indonesia, Jakarta, Indonesia.  0000-0002-0783-7052

<sup>2</sup>Department of Orthodontics, Faculty of Dentistry, Universitas Indonesia, Jakarta, Indonesia.  0000-0002-2535-3983

<sup>3</sup>Department of Orthodontics, Faculty of Dentistry, Universitas Indonesia, Jakarta, Indonesia.  0000-0002-8072-3967

Author to whom correspondence should be addressed: Retno Widayati, Department of Orthodontics, Faculty of Dentistry, Universitas Indonesia, Jalan Salemba Raya no. 4, 10430, Jakarta, Indonesia. Phone: +62 811965364. E-mail: [widayati22@yahoo.com](mailto:widayati22@yahoo.com).

Academic Editors: Alessandro Leite Cavalcanti and Wilton Wilney Nascimento Padilha

Received: 22 February 2019 / Accepted: 17 June 2019 / Published: 01 July 2019

### Abstract

**Objective:** To evaluate the differences in the stress distribution on the upper first molar with and without transpalatal arch and a second molar when a 150 g force is applied during canine distalization using finite element analysis. **Material and Methods:** We constructed several models with data obtained by scanning human skulls using cone beam computed tomography. A robust three-dimensional maxillary model was then constructed by assembling the previously completed robust models of the maxilla and second molar with and without transpalatal arch, and canine distalization was simulated using a 150 g force. The data consisted of color spectrum figures representing the stress distribution. **Results:** For the upper first molar and its alveolar bone, there was a statistically significant difference in the stress distribution between the upper first molar with transpalatal arch, the upper first molar without transpalatal arch, and the upper first molar with transpalatal arch and a second molar as reinforcement. **Conclusion:** Stress distribution on the first molar and alveolar bone, indicated by the maximum and minimum principal stress, as well as the pressure von Mises, exhibited a similar pattern. The highest amount of stress was observed in the model of the first molar without transpalatal arch, followed by the model of the first molar with transpalatal arch and, finally, the model of the first molar with transpalatal arch and a second molar.

**Keywords:** Investigative Techniques; Orthodontics; Cone-Beam Computed Tomography.

## Introduction

The transpalatal arch (TPA) is an orthodontic device that is used to strengthen anchorage. Whether the use of TPA and a second molar as reinforcement anchorage can reduce stress remains unclear. Reducing the stress distribution is thought to reduce the anchorage loss, and some clinicians believe that TPA prevents the loss of anchorage [1-3]. However, it was previously reported that TPA does not significantly affect anchorage [4,5]. In order to determine the amount of stress in the presence and absence of TPA and when TPA is combined with a second molar, it is necessary to understand the stress distribution in the upper first molar where the TPA is placed, as well as the stress on the alveolar bone around the tooth. Some authors measured the stress on the first molar while splinting with a TPA and reported that TPA can reduce the stress distribution on the first molar and prevent molar rotation [6,7].

Anchorage depends on periodontal stress, and TPA can modify the stress distribution applied to the molars and surrounding tissue. Unfortunately, it is impossible to measure human periodontal stress distributions in vivo; therefore, an alternative approach that uses three-dimensional (3D) simulation and finite element analysis (FEA) was developed [6-8].

FEA has been used to measure the stress distribution during orthodontic treatment for over two decades [9,10]. This technique involves the use of computer-aided design to calculate the biochemical system and pressure distribution as well as study the relationship between tooth movement, root resorption, and bone remodeling. Using this mathematical method, a geometric structure is simulated on a computer along with its mechanical properties [9-11].

Here, we conducted a skull scan using cone beam computed tomography (CBCT) and then created a solid model of the teeth, TPA, root teeth, alveolar bone, bracket, and archwires according to the mechanical properties determined from Young's modulus and Poisson's ratio. A solid model was assembled and a 150 g canine distalization force was applied. The pressure distribution measurements were performed by measuring the main pressure on the x-, y-, and z-axis, representing the maximum principal stress (MaxPS), minimum principal stress (MinPS), and pressure von Mises (VonMS).

We sought to compare the stress distribution for MinPS, MaxPS, and VonMS on the upper first molar and the alveolar bone with and without TPA and on the upper second molar while applying a 150 g canine distalization force.

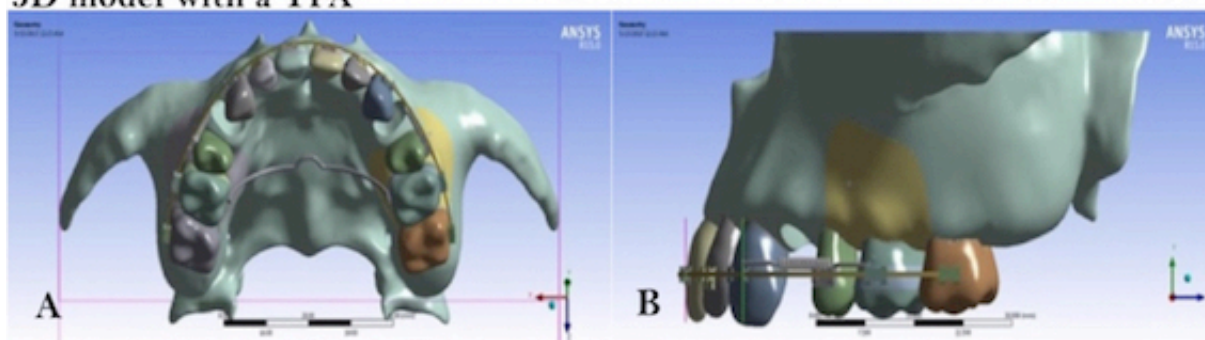
## Material and Methods

The FEA calculations were performed using ANSYS 15.0 (Ansys Inc., Canonsburg, PA, USA). Model construction began after the human skull was scanned using CBCT. The results of the scan were saved on a CD in a DICOM format, and a robust model was constructed using Geomagic software by assembling every tooth and its alveolar bone [12]. We constructed a bracket, a force module, an archwire, a molar band, and a TPA on the basis of real models using Autodesk Inventor software. A robust 3D maxillary model was then constructed by assembling the previously

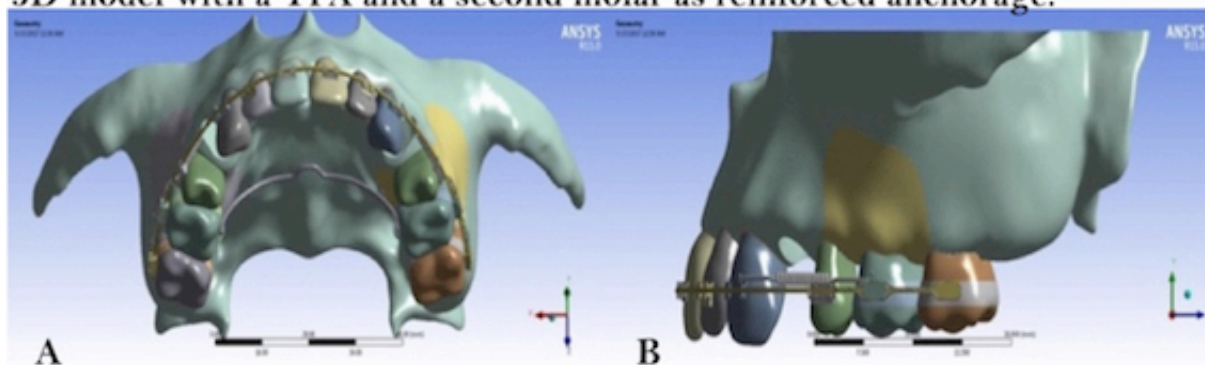
completed robust models. For the arch form guideline, we used a 0.019" × 0.025" archwire, a natural incline, good alignment, and mirrors to construct a complete two-quadrant 3D model [9].

We created three robust models: a 3D maxillary model with a TPA (Figure 1), a 3D maxillary model with a TPA and an upper second molar (Figure 2), and a 3D maxillary model without a TPA (Figure 3). Automeshing was accomplished using ANSYS.

### 3D model with a TPA



### 3D model with a TPA and a second molar as reinforced anchorage.



### 3D model without a TPA

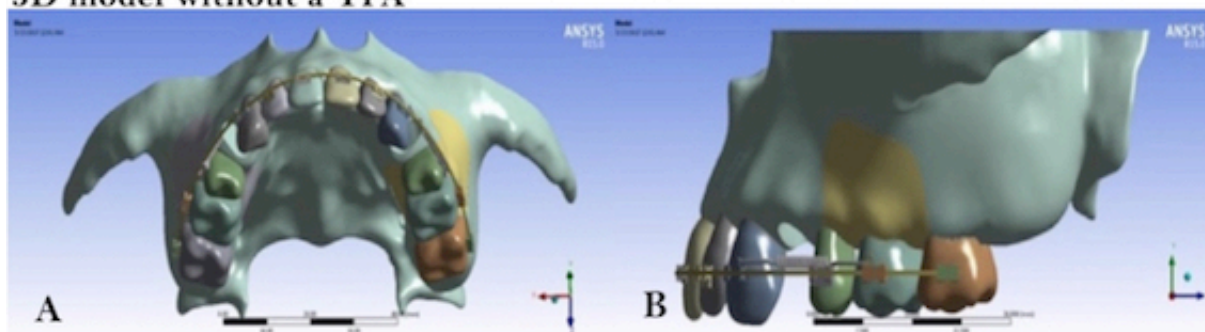


Figure 1. 3D maxillary models. (A) Occlusal view and (B) Sagittal view.

The finite element model structures included a tooth, a periodontal ligament, an alveolar bone, a bracket, an archwire, and steel (TPA). Each composition exhibited a different mechanical property previously reported in the literature. All materials were homogenous and isotropic [9].

The boundary condition on the 3D maxillary model was 0° of movement in all directions and on all peripheral nodes. All three models were subjected to a 150 g canine distalization force using ANSYS software. Each model was analyzed three times to determine the compressive stress

(MinPS), the area with the largest shear when forces are applied (tensile stress, MaxPS), and the material's elasticity until permanent deformation (VonMS) [11].

## Results

Finite element outputs can be examined qualitatively and quantitatively. As shown in Figures 2 and 3, stress distributions were qualitatively evaluated using a series of colors, as shown in the color spectrum on the left side of the images, where red represents the highest amount of stress and blue represents the lowest amount of pressure.

MinPS analysis on the First Molar of all three models revealed a similar color pattern, with the highest stress distribution at the root apex. Figure 2 shows that the addition of anchorage and the second molar reduced the stress distribution, as the red area appears to be smaller in this model. The highest MaxPS on the First Molar was in the model without TPA and was located at the distopalatal apex. The color pattern was similar to that for MinPS, and the stress distribution was smaller in the 3D model with a TPA and a second molar. The stress distribution for VonMS on the First Molar also exhibited a similar color pattern. The highest stress distribution was in the 3D model without a TPA, and the lowest was in the 3D model with a TPA and a second molar.

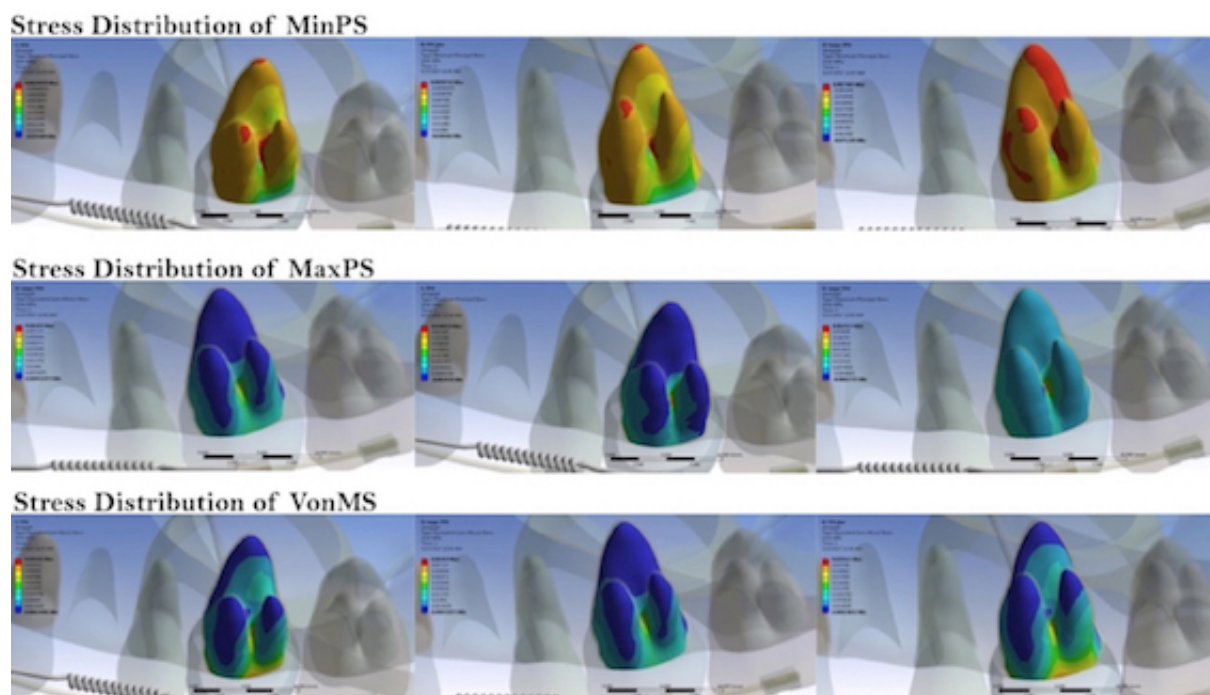
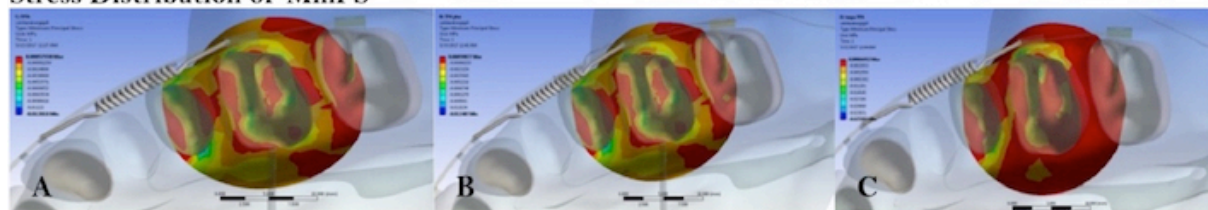


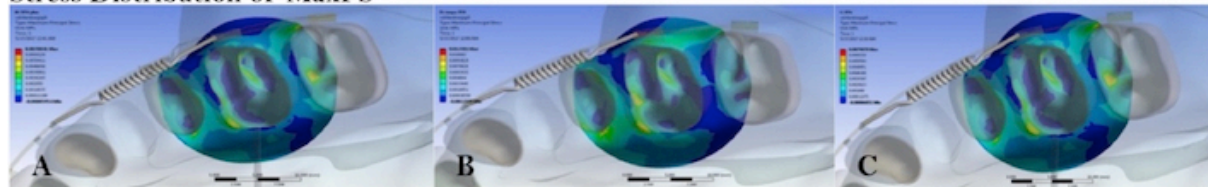
**Figure 2.** Color patterns showing the stress distribution of MinPS, MaxPS and VonMS on the first molar. (A) 3D model with a TPA. (B) 3D model with a TPA and a second molar as reinforced anchorage. (C) 3D model without a TPA.

The color patterns for MinPS, MaxPS, and VonMS around the alveolar bone of the first molar were similar. Color intensity differences showed a reduction in the stress distribution on the TPA and TPA with second molar models with reinforced anchorage (Figure 3).

**Stress Distribution of MinPS**



**Stress Distribution of MaxPS**



**Stress Distribution of VonMS**

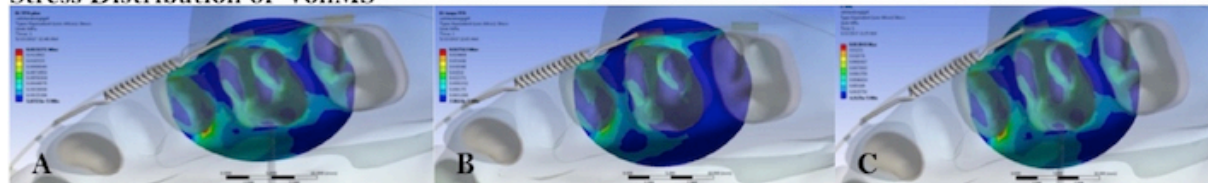


**Figure 3.** Color patterns showing the stress distribution of MinPS, MaxPS and VonMS on the first molar alveolar bone. (A) 3D model with a TPA. (B) 3D model with a TPA and a second molar as reinforced anchorage. (C) 3D model without a TPA.

The model with TPA and a second molar as reinforcement had the lowest MaxPS (0.0017 MPa). The highest MaxPS was found in the model without TPA (0.00219 MPa). The model with TPA and a second molar had the lowest VonMS (0.00259 MPa), followed by the model with TPA (0.02134 MPa) and, finally, the model without TPA (0.02189 MPa) (Table 1).

**Table 1.** Differences in the stress distribution (MinPS, MaxPS, and VonMS) for the 3D models of the first molar.

3D Model	Reinforced Anchorage						p-value
	TPA		TPA and Second Molar		Without TPA		
	Mean	SD	Mean	SD	Mean	SD	
MinPS	0.00177	0.00062	0.02189	0.00143	0.00357	0.00158	<0.001*
MaxPS	0.00196	0.00134	0.00170	0.00060	0.02198	0.00281	<0.001*
VonMS	0.02134	0.00131	0.00259	0.00084	0.02189	0.00143	<0.001*

\*Statistically Significant; SD: Standard Deviation.

The highest stress distributions (MinPS, MaxPS, and VonMS) on the alveolar bone were found in the model without TPA (Table 2).

**Table 2.** Differences in the stress distribution (MinPS, Max PS, and VonMS) for the 3D models of the alveolar bone.

Alveolar Bone	Reinforced Anchorage						p-value
	TPA		TPA and Second Molar		Without TPA		
	Mean	SD	Mean	SD	Mean	SD	
MinPS	0.00044	0.00006	0.00035	0.00009	0.00045	0.00007	<0.001*
MaxPS	0.00635	0.00043	0.00617	0.00051	0.00899	0.00062	<0.001*
VonMS	0.01055	0.00116	0.01016	0.00111	0.01859	0.00274	<0.001*

\*Statistically Significant; SD: Standard Deviation.

## Discussion

Some studies have questioned the use of TPA as reinforced anchorage during orthodontic treatment with distalized canine teeth [4,5]. TPA can redistribute the stress applied to a tooth and its supporting tissue [8]. Quantification of these stress distributions requires a 3D model using FEA as an alternative to the invasive method that has been predominant for over two decades. The results of FEA can be depicted both qualitatively and quantitatively. Qualitative depictions involve color patterns and are based on the color plot on the left side of the display, whereas quantitative depictions use the mean stress values (MinPS, MaxPS, and VonMS).

MinPS analysis of all models used in this study showed a similar color pattern for the compressive stress. The mesiobuccal, distobuccal, and palatal root of the first upper molar received some of the stress, but the highest amount of stress was distributed on the root apex. Figure 2 shows the reduction of stress distribution with anchorage reinforcement. This reduction is indicated by reductions in the red color. All of the alveolar bone surrounding the first upper molar in the cervical region exhibited the same stress distribution pattern. Figure 3 shows a less red color in the model without a TPA. Thus, the mean compressive stress value on the alveolar bone molar corresponded to the color patterns in the 3D models (Table 2).

Orthodontic treatment forces can impose stress on the tooth and alveolar bone. This means that resorption and deposition occur under an area of increased pressure and tension. Previous authors analyzed the stress distributions on canine teeth distalized with a force of 150 g and found that the highest amount of stress was located in the cervical region and that the stress distribution was higher at the root compared to the alveolar bone [13]. These results agreed with those previously reported [13].

MaxPS, which indicates the area with the largest shear when a force is applied, was also reduced with reinforced anchorage. These qualitative results are similar to the color patterns depicted in Figure 2.

Similar to the other parameters measured, the material's elasticity until permanent deformation, represented by VonMS, was reduced with reinforced anchorage. These results are in accordance with the color patterns shown in Figure 2. MinPS, MaxPS, and VonMS all exhibited a similar stress pattern on the alveolar bone.

There is a significant difference in the distribution of stress (MinPS, MaxPS, and VonMS) between the models for the first molar and TPA, the first molar and TPA with a second molar as reinforcement, and the first molar without TPA (Tables 1 and 2). The highest stress distributions (MinPS, MaxPS, and VonMS) on the first molar (Table 1) and the alveolar bone (Table 2) were found in the model without TPA, followed by the model with TPA and, finally, the model with TPA and a second molar as reinforcement. The results of the study are in accordance with the theory that reinforced anchorage will reduce stress and also reduce the loss of anchorage.

The mean stress distributions (MinPS, MaxPS, and VonMS) for the model without TPA were significantly larger than those for the model with TPA. There were significant differences in

the stress distributions for the 3D models (Table 2). TPA reduced the stress on the upper first molar, affirming its function as a reinforced anchor. The average stress distribution value for the alveolar bone around the root of the upper first molar showed a similar trend (Table 2). If orthodontic movement requires a strong anchor, it is advisable to use TPA and the upper second molar during canine teeth distalization. Our results differed from other authors who reported that TPA did not exert significant effects during reinforced anchorage [4,5]

The highest VonMS value on the first molar, both on the tooth and on the alveolar bone, was found in the model without TPA, followed by the models with TPA and TPA with a second molar [10]. A previous study showed that the highest amount of stress (0.0026 N/mm<sup>2</sup>) was in the cervical area. Importantly, the stress of this magnitude can impose strain on capillary blood vessels, and pressure on the capillary blood vessels marks the beginning of the remodeling process [9].

In the previous report, stress values on the 3D model with and without TPA when subjected to mesial forces were compared. The result showed a 1 : 4 ratio for the stress without TPA versus that with TPA. This means that TPA can reduce the loss of anchorage in the AP direction by four orders of magnitude during initial movement [8]. Begum reported that TPA prevented molar rotation during initial movement, and Raucci stated that TPA could prevent molar tipping and rotation [1,6]. Mesial forces subjected to TPA can cause molar tipping, but the tipping angle was similar to that for the models with and without TPA. However, molar rotation and anterior movement were found in the model without TPA [7].

This report suggests that the use of TPA and a second molar as a reinforced anchorage during canine distalization decreases the stress distribution on the tooth and alveolar bone. However, findings vary regarding the use of TPA. This may be due to the theoretical limitations of biological model construction. Each tissue possesses specific characteristics, and differences are found according to bone density, trabecula, periodontal ligaments, age, and gender.

## Conclusion

Stress (MinPS, MaxPS, and VonMS) on the first molar was focused on the root apex and that on the alveolar bone was focused on the cervical area. The distribution for both areas exhibited similar patterns. The highest stress distributions (MinPS, MaxPS, and VonMS) on the first molar and alveolar bone were found in the model without TPA, followed by the models with TPA and TPA with a second molar as reinforcement.

**Authors' Contributions:** PBP contributed to conception and data design, performed the experiment, analysis, and interpretation and wrote the manuscript. RW designed the study and critically revised the manuscript. MP critically revised the manuscript.

**Financial Support:** None.

**Conflict of Interest:** The authors declare no conflicts of interest.

**Acknowledgment:** The authors thank Model Simulasi for providing help in generating the 3D model and simulation. The authors are also grateful to drg. Erwin Siregar, Sp.Ort (K), Dr. drg. Miesje K. Purwanegara, SU, Sp.Ort (K), and drg. Krisnawati, Sp. Ort (K) for critically reviewing this study.

## References

- [1] Raucci G, Pachêco-Pereira C, Grassia V, D'Apuzzo F, Flores-Mir C, Perillo L. Maxillary arch changes with transpalatal arch treatment followed by full fixed appliances. *Angle Orthod* 2014; 85(4):683-9. <https://doi.org/10.2319/070114-466.1>
- [2] Feldmann I, Bondemark L. Anchorage capacity of osseointegrated and conventional anchorage systems: a randomized controlled trial. *Am J Orthod Dentofacial Orthop* 2008; 133(3):19-28. <https://doi.org/10.1016/j.ajodo.2007.08.014>
- [3] Alhadlaq A, Alkhadra T, El-Bialy T. Anchorage condition during canine retraction using transpalatal arch with continuous and segmented arch mechanics. *Angle Orthod* 2016; 86(3):380-5. <https://doi.org/10.2319/050615-306.1>
- [4] Jacobson A. Retrospective cephalometric investigation of the effects of soldered transpalatal arches on the maxillary first molars during orthodontic treatment involving extraction of maxillary first bicuspids. *Am J Orthod Dentofacial Orthop* 2006; 129(1):81. <https://doi.org/10.1016/j.ajodo.2005.05.021>
- [5] Zablocki HL, McNamara JA, Franchi L, Baccetti T. Effect of the transpalatal arch during extraction treatment. *Am J Orthod Dentofacial Orthop* 2008; 133(6):852-60. <https://doi.org/10.1016/j.ajodo.2006.07.031>
- [6] Begum MS, Dinesh MR, Amarnath BC, Dharma RM, Prashanth CS, Shetty KA, et al. Comparison of the effect of transpalatal arch on periodontal stress and displacement of molars when subjected to orthodontic forces. A finite element analysis. *Br J Med Dent Res* 2016; 12(12):1-7. <https://doi.org/10.9734/BJMMR/2016/22500>
- [7] Bobak V, Christiansen RL, Hollister SJ, Kohn DH. Stress-related molar responses to the transpalatal arch: A finite element analysis. *Am J Orthod Dentofacial Orthop* 1997; 112(5):512-8. [https://doi.org/10.1016/S0889-5406\(97\)90100-1](https://doi.org/10.1016/S0889-5406(97)90100-1)
- [8] Kojima Y, Fukui H. Effects of the transpalatal arch on molar movement produced by mesial force: A finite element simulation. *Am J Orthod Dentofacial Orthop* 2008; 134(3):335.e1-7. <https://doi.org/10.1016/j.ajodo.2008.03.011>
- [9] Knop L, Gandini L, Shincovsk RL, Gandini MREAS. Scientific use of the finite element method in Orthodontics. *Dent Press J Orthod* 2015; 20(2):119-25. <https://doi.org/10.1590/2176-9451.20.2.119-125.sar>
- [10] Mehta F, Joshi H. Finite element method: An overview. *IOSR J Dent Med Sci* 2016; 15(3):38-41.
- [11] Mohammed S, Desai H. Basics concepts of finite element analysis and its application in dentistry: An overview. *J Oral Hyg Health* 2014; 2(5):156-60. <https://doi.org/10.4172/2332-0702.1000156>
- [12] Penedo ND, Elias CN, Pacheco MCT, Gouvêa JP. 3D simulation of orthodontic tooth movement. *Dent Press J Orthod* 2010; 15(5):98-108. <https://doi.org/10.1590/S2176-94512010000500012>
- [13] Jing Y, Han XL, Cheng B, Bai D. Three-dimensional FEM analysis of stress distribution in dynamic maxillary canine movement. *Chinese Sci Bull* 2013; 58(20):2454-9. <https://doi.org/10.1007/s11434-013-5729-y>